

Conference on High Energy Physics 1972, Chicago, Illinois (unpublished).

<sup>12</sup>R. P. Feynman, M. Kislinger, and F. Ravndal, Phys. Rev. D 2, 2706 (1971).

<sup>13</sup>G. Gustafson, Nucl. Phys. B40, 205 (1972).

<sup>14</sup>F. E. Close and F. J. Gilman, Phys. Letters 38B, 541 (1972); F. E. Close, F. J. Gilman, and I. Karliner, Phys. Rev. D 6, 2533 (1972).

PHYSICAL REVIEW D

VOLUME 7, NUMBER 3

1 FEBRUARY 1973

## Linear Regge Trajectories with a Left-Hand Cut

N. G. Antoniou\*  
CERN, Geneva, Switzerland

and

C. G. Georgalas and C. B. Kouris  
Nuclear Research Center "Democritus," Aghia Paraskevi Attikis, Greece  
(Received 14 June 1972)

The properties of boson Regge trajectories  $\alpha(s)$  with a left-hand cut for  $s < 0$  are studied, with the following assumptions: (a)  $\text{Re}\alpha(s)$  is linear in the physical regions of the  $s$  and  $t$  channels. (b) The imaginary part is asymptotically smaller than the real part. (c) At  $s = 0$ ,  $\alpha(s)$  has a branch point due to the existence of a Regge cut  $\alpha_c(s)$  in the angular momentum plane, with  $\alpha_c(0) = \alpha(0)$ . The branch point is attributed to the collision of the physical pole  $\alpha(s)$  with a second-sheet pole  $\tilde{\alpha}(s)$ , at  $s = 0$ . (d) The function  $\alpha(s)$  is analytic in the  $s$  plane. Under these assumptions the imaginary part for each boson trajectory is obtained in terms of a parameter  $A$  and a parameter-free universal function determined by solving an integral equation numerically. The parameter  $A$  is determined by requiring that the first meson of each trajectory have the observed width. The model gives imaginary parts increasing almost linearly with  $s$  for large  $|s|$ . The widths of the recurrences increase linearly with their mass. The results support exchange degeneracy  $\rho$ - $f$ ,  $K^*$ - $K_N$ ,  $\omega$ - $A_2$ . The imaginary part, for  $s < 0$ , is compared with the phenomenological results of other authors.

### I. INTRODUCTION

The possibility that Regge poles  $\alpha(s)$  are complex for  $s < 0$  has been investigated recently.<sup>1-3</sup> This means that Regge trajectories develop a left-hand cut for  $s < 0$ . The mechanism of production of this cut is the collision of two Regge poles.<sup>1,2</sup> In relativistic scattering the mechanism of generating complex poles is strongly related to the existence of cuts in the angular momentum plane. The colliding poles are expected, on physical grounds, to lie on different Riemann sheets of the angular momentum plane for  $s > 0$ , whereas for  $s < 0$  they are complex conjugates of each other on the same sheet, which is assumed in this paper to be the physical (first) sheet. There is therefore a strong pole-cut relationship based on analyticity in the angular momentum plane.<sup>2</sup> Hence the study of complex poles is connected to the investigation of the properties of the Regge cuts. In particular, it turns out that the effect of Regge cuts can be simulated by a pair of complex poles in a satisfactory way.<sup>1</sup>

The new quantity entering into the Regge-pole description of the high-energy two-body reactions in the complex-pole model is the imaginary part of the trajectory  $\alpha_I(s)$ , along the left-hand cut ( $s < 0$ ). The form of the function  $\alpha_I(s)$  is unknown and only a crude phenomenological determination can be achieved. On the other hand, since the nature of the cuts in the angular momentum plane is not yet known in detail, any information for  $\alpha_I(s)$  from the pole-cut relationship is necessarily model-dependent.

In the present work an integral equation for the discontinuity function has been established by the use of analyticity in the  $s$  plane together with some general properties of Regge poles and cuts. The solution of this equation is then determined numerically and the results are compared with the widths of the boson recurrences and with the phenomenological left-hand absorptive part.

In Sec. II the assumptions are stated and the equations of the model are derived and discussed. In Sec. III our results are compared with the experimental data and the phenomenological results

of other authors. In Sec. IV the conclusions are briefly discussed.

## II. THE MODEL

We consider a generic boson trajectory  $\alpha(s)$  for which we make the following assumptions:

(a) The trajectory  $\alpha(s)$  is analytic in the  $s$  plane with two cuts  $-\infty < s < s_L$  and  $s_0 < s < \infty$ , where  $s_0$  is the lowest threshold for the trajectory and  $s_L$  is the point where  $\alpha(s)$  collides with a second-sheet pole in the  $l$  plane.<sup>4</sup>

(b) The cut is weak and  $s_L$  approximately coincides with zero owing to the property  $\alpha_c(0) = \alpha(0)$ , where  $\alpha_c(s)$  is the absorptive cut associated with the pole  $\alpha(s)$ . In the case we consider, both the  $l$ -plane and the  $s$ -plane branch points lie on the real axis. It follows then from the analysis of Ref. 2 that the threshold behavior of the imaginary part of  $\alpha(s)$  for  $s < 0$  is  $\alpha_I(s) \sim (-s)^{3/2}$ ,  $s \rightarrow 0_-$ .

The available information regarding the behavior at the physical threshold  $s = s_0$  is rather ambiguous because it comes from nonrelativistic arguments (potential scattering) and it relies heavily on the value of the intercept  $\alpha(0)$ .<sup>5</sup> Moreover, the exact threshold behavior at  $s = s_0$  suggested by potential scattering is not consistent in general with our assumption (c) below, that the  $\text{Re}\alpha(s)$  is linear.<sup>6</sup>

On the contrary, near the left-hand threshold the trajectory is known to behave like<sup>2</sup>

$$\alpha_{1,2}(s) \approx \alpha(0) + \alpha s \pm b s^{3/2} + \dots,$$

which is consistent with linearity of the real part. We therefore consider it more safe to assume

at the beginning only the threshold behavior at  $s \rightarrow 0_-$ .

We shall see later that a behavior  $(s - s_0)^{1/2}$  at the physical threshold can be deduced from our assumptions for  $\text{Im}\alpha(s)$ .

(c) The real part,  $\alpha_R(s)$ , of the trajectory is linear in the physical regions of both  $s$  and  $t$  channel ( $s > s_0$  and  $s < 0$ ) as suggested by the phenomenological study of the Regge poles. In general the two linear parts (for  $s > s_0$  and  $s < 0$ ) may be parallel but they do not necessarily coincide, since a small splitting is not excluded by the data.

Hence we write

$$\begin{aligned} \text{Re}\alpha(s) &= \alpha^R + b^R s \quad (s > s_0), \\ \text{Re}\alpha(s) &= \alpha^L + b^L s \quad (s < 0). \end{aligned} \quad (1)$$

(d) The imaginary part  $\text{Im}\alpha(s)$  for  $s > s_0$  satisfies the relation  $\text{Im}\alpha(s) \lesssim s^{1-\epsilon}$  for  $s \rightarrow \infty$ .

This hypothesis is less stringent than it may seem. In fact,  $\alpha(s) \sim s$  for  $s \rightarrow +\infty$ , as will be discussed in detail in the Appendix. This implies  $\text{Im}\alpha(s) \lesssim s$ . Our assumption (d) therefore only excludes the possibility  $\epsilon = 0$ .

Technically, this implies square integrability of the function  $f(u)$  defined by Eq. (14) below. Physically, however, for sufficiently small  $\epsilon$ , the deviation of  $\text{Im}\alpha(s)$  from linearity may not even be observable. In fact, our explicit calculation will show that asymptotically,  $\text{Im}\alpha(s)$  does not differ appreciably from linearity.

Using these assumptions we write once-subtracted dispersion relations for the functions  $F_1(s) = \alpha(s)/\sqrt{s}$  and  $F_2(s) = \alpha(s)/(s_0 - s)^{1/2}$ . Denoting by  $\alpha_I(s)$  and  $\text{Im}\alpha(s)$  the imaginary parts of  $\alpha(s)$  for  $s < 0$  and  $s > s_0$ , respectively, we obtain

$$\frac{\alpha_I(s)}{\sqrt{-s}} = \frac{\alpha_R(s_1)}{\sqrt{s_1}} + \frac{s - s_1}{\pi} P \int_{s_0}^{\infty} \frac{\text{Im}\alpha(s') ds'}{(s' - s)(s' - s_1)\sqrt{s'}} - \frac{s - s_1}{\pi} P \int_{-\infty}^0 \frac{(\alpha^L + b^L s') ds'}{(-s')^{1/2}(s' - s)(s' - s_1)} \quad (s < 0), \quad (2)$$

$$-\frac{\text{Im}\alpha(s)}{(s - s_0)^{1/2}} = \frac{\alpha_R(s_1)}{(s_0 - s_1)^{1/2}} + \frac{s - s_1}{\pi} P \int_{s_0}^{\infty} \frac{(\alpha^R + b^R s') ds'}{(s' - s_0)^{1/2}(s' - s)(s' - s_1)} + \frac{s - s_1}{\pi} P \int_{-\infty}^0 \frac{\alpha_I(s') ds'}{(s_0 - s')^{1/2}(s' - s)(s' - s_1)} \quad (s > s_0), \quad (3)$$

where  $0 < s_1 < s_0$ . For simplicity we take  $s_1 = \frac{1}{2}s_0$ .

Equations (2) and (3) are coupled integral equations for the unknown functions  $\alpha_I(s)$  and  $\text{Im}\alpha(s)$ . Substituting the expression (2) for  $\alpha_I(s)$  in (3) we finally obtain the following linear integral equation:

$$\phi(s) = \phi_0(s) + \int_{s_0}^{\infty} G(s, s'') \phi(s'') ds'' \quad (s > s_0), \quad (4)$$

where

$$\phi(s) = \frac{\text{Im}\alpha(s)}{(s - \frac{1}{2}s_0)(s - s_0)^{1/2}}, \quad (5)$$

$$\phi_0(s) = \frac{A}{2(s - \frac{1}{2}s_0)} + \frac{B\sqrt{s}}{\pi(s - \frac{1}{2}s_0)(s - s_0)^{1/2}} \ln \left( \frac{\sqrt{s} + (s - s_0)^{1/2}}{\sqrt{s} - (s - s_0)^{1/2}} \right), \tag{6}$$

$$G(s, s'') = \frac{1}{\pi^2} \left( \frac{s'' - s_0}{s''} \right)^{1/2} \frac{1}{s'' - s} \left[ \left( \frac{s}{s - s_0} \right)^{1/2} \ln \left( \frac{\sqrt{s} - (s - s_0)^{1/2}}{\sqrt{s} + (s - s_0)^{1/2}} \right) - \left( \frac{s''}{s'' - s_0} \right)^{1/2} \ln \left( \frac{\sqrt{s''} - (s'' - s_0)^{1/2}}{\sqrt{s''} + (s'' - s_0)^{1/2}} \right) \right]. \tag{7}$$

The constants  $A$  and  $B$  are

$$A = \left( \frac{2}{s_0} \right)^{1/2} \left[ (2\alpha^R - \alpha^L) + \frac{1}{2}s_0(2b^R - b^L) - \alpha(\frac{1}{2}s_0) \right], \tag{8}$$

$$B = \left( \frac{2}{s_0} \right)^{1/2} \left[ \alpha^L + \frac{1}{2}b^L s_0 - \alpha(\frac{1}{2}s_0) \right]. \tag{9}$$

From Eqs. (2) and (9) we have

$$\alpha_I(s) = \sqrt{-s} \left( -B + \frac{s - \frac{1}{2}s_0}{\pi} \int_{s_0}^{\infty} \frac{\text{Im}\alpha(s') ds'}{(s' - s)(s' - \frac{1}{2}s_0)\sqrt{s'}} \right). \tag{10}$$

The threshold behavior  $\alpha_I(s) \sim (-s)^{3/2}$  leads then to the condition

$$B = -\frac{s_0}{2\pi} \int_{s_0}^{\infty} \frac{\text{Im}\alpha(s') ds'}{(s' - \frac{1}{2}s_0)(s')^{3/2}}. \tag{11}$$

Substituting (11) into (6) and introducing the new variables

$$u = \left( \frac{s - s_0}{s} \right)^{1/2}, \quad v = \left( \frac{s'' - s_0}{s''} \right)^{1/2},$$

we transform (4) into the following integral equation:

$$f(u) = 1 + \int_0^1 \tilde{K}(u, v) f(v) dv, \tag{12}$$

where

$$\begin{aligned} \tilde{K}(u, v) = & \frac{2v^2}{\pi^2(v^2 - u^2)(1 + v^2)} \\ & \times \left[ \left( \frac{1 + v^2}{u} \right) \ln \frac{1 - u}{1 + u} - \left( \frac{1 + u^2}{v} \right) \ln \frac{1 - v}{1 + v} \right], \end{aligned} \tag{13}$$

and  $f(u)$  is defined by

$$\text{Im}\alpha(s) = \frac{1}{2} A (s - s_0)^{1/2} f(u). \tag{14}$$

The quantity  $\alpha_I$  is then given by the relation

$$\alpha_I(w) = \frac{A\sqrt{s_0}}{\pi(w^2 - 1)^{1/2}} \int_0^1 \frac{u^2 f(u) du}{u^2 - w^2}, \tag{15}$$

where

$$w = \left( \frac{s - s_0}{s} \right)^{1/2} \quad (s < 0).$$

The kernel (13) is square-integrable but not

bounded and has no singularity at  $u = v$ . Equation (12) has therefore a unique solution in  $L^2$ , which we determine numerically. The assumption that the solution  $f(u)$  is square-integrable is equivalent to assuming  $\text{Im}\alpha(s) \lesssim s^{1-\epsilon}$  for large  $s$ .<sup>7</sup>

The solution has been obtained (a) by the Fredholm method (approximation by a system of linear algebraic equations) and (b) by the method of successive iterations. The second method is applicable since our kernel is an  $L^2$  kernel,  $\phi_0(u) = 1$ , is a square-integrable function in the interval  $[0, 1]$  and  $\|K(u, v)\| < 1$ . The results of both methods coincide and the function  $f(u)$  thus obtained is shown in Fig. 1.

### III. RESULTS AND COMPARISON WITH DATA

The function  $f(u)$  has a universal character for all boson trajectories. From the fact that  $f(u)$  tends to a constant for  $u \rightarrow 0$  or  $s \rightarrow s_0$  and from Eq. (14) we obtain a behavior  $\text{Im}\alpha(s) \sim (s - s_0)^{1/2}$  near the physical threshold.

The  $\text{Im}\alpha(s)$  given by (14) has been determined for each trajectory ( $\rho, \omega, K^*$ ) from Eq. (14) by the requirement that the first meson of each trajectory have the experimental width. We observe that the  $\text{Im}\alpha(s)$  increases almost linearly with  $s$ . The results are shown in Fig. 2. The model gives then the following expression for the width function:

$$\Gamma(s) = \frac{\text{Im}\alpha(s)}{b^R \sqrt{s}}. \tag{16}$$

The results are shown in Fig. 3, plotted along

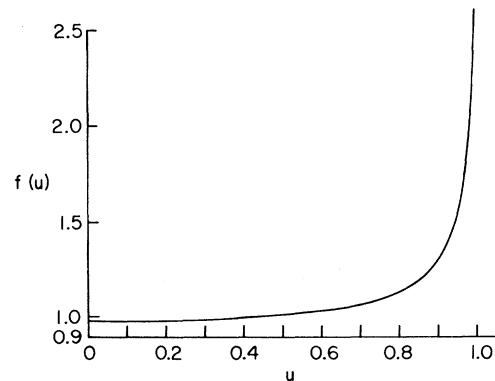


FIG. 1. Plot of the universal function  $f(u)$ .

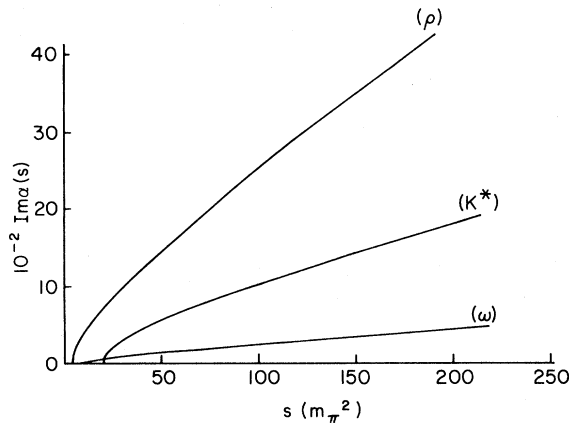


FIG. 2. The imaginary part of  $\alpha(s)$  for  $s > s_0$  as a function of  $s$  for the boson trajectories  $\rho$ ,  $\omega$ , and  $K^*$ .

with the experimental widths.

We observe that the widths of  $f$ ,  $A_2$ , and  $K_N(1420)$  resonances lie in the neighborhood of the curves of  $\rho$ ,  $\omega$ , and  $K^*$ , respectively. The picture suggests exchange degeneracy between the trajectories  $\rho$ - $f$ ,  $\omega$ - $A_2$ , and  $K^*$ - $K_N$ .

We observe in particular that a split  $A_2$  resonance with two narrow components fits well into the  $\omega$  curve whereas a single large width  $A_2$  (100 MeV) favors  $\rho$ - $A_2$  degeneracy. We remark that a nonzero  $\text{Im}\alpha$  splits the exchange-degenerate bosons  $\rho$ ,  $\omega$ ,  $f$ , and  $A_2$  in two groups ( $\rho$ - $f$  and  $\omega$ - $A_2$ ).

In Fig. 4 we plot  $\alpha_I(s)$  as a function of  $s$  for the trajectories  $\rho$ ,  $\omega$ , and  $K^*$  using formula (15). In the same figure we plot for comparison the phenomenological form of  $\alpha_I$  for the  $\rho$  trajectory found in Refs. 8 and 9 from the analysis of  $\pi N$  charge-exchange scattering. The difference of the two phenomenological curves suggests that it is difficult to extract reliably  $\alpha_I(s)$  from phenomenological analysis of the data since the results depend dras-

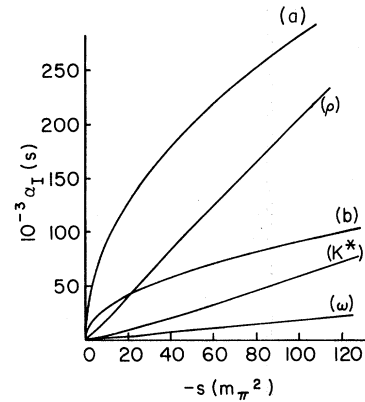


FIG. 4. The imaginary part of  $\alpha(s)$  for  $s < 0$  as a function of  $s$  for the trajectories  $\rho$ ,  $\omega$ , and  $K^*$ . The phenomenological curves for the  $\rho$  trajectory found in (4) (curve a) and in (5) (curve b) are also plotted for comparison.

tically on the choice of parametrization.

We observe that  $\alpha_I(s)$  for the  $\omega$  trajectory is considerably smaller than those of  $\rho$  and  $K^*$  due to the small value of the  $\omega$  width.

The condition that the first meson of each trajectory must have the observed width determines  $A/b^R$ . For example, for  $\rho$ , we find

$$\frac{A}{b^R} = 0.0274 m_\pi^{-1},$$

which by (11) and (14) leads to

$$\frac{B}{b^R} = -0.00227 m_\pi^{-1}.$$

Using these results one can relate the  $\alpha(\frac{1}{2}s_0)$  to the intercepts and slopes of the trajectories [Eqs. (8) and (9)]. With reasonable phenomenological values for these parameters one finds an estimate of  $\alpha(\frac{1}{2}s_0)$  near the values of the intercepts.

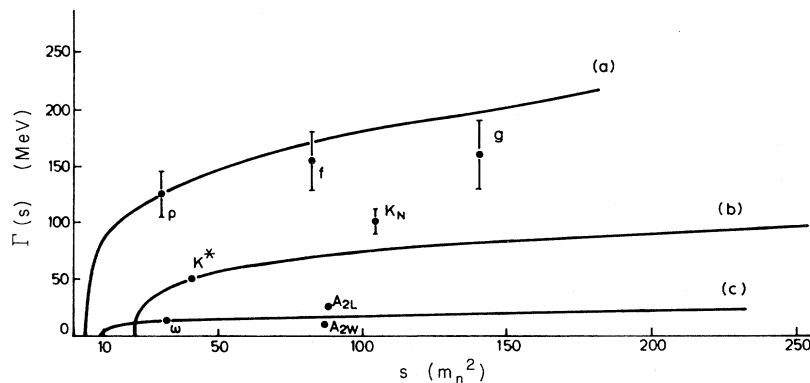


FIG. 3. The width function  $\Gamma(s)$  for the  $\rho$ ,  $\omega$ , and  $K^*$  trajectories plotted as a function of  $s$  along with the experimental widths of the  $\rho$ ,  $f$ ,  $g$ ,  $\omega$ ,  $A_2$ ,  $K^*$ , and  $K_N$  particles.

## IV. CONCLUSIONS

With some general assumptions concerning the behavior of boson trajectories with a left-hand cut we have written two coupled integral equations for the imaginary parts of  $\alpha(s)$  in the regions  $s > s_0$ ,  $s < 0$ . These equations lead to expressions for the imaginary parts and the width functions in terms of a universal parameter-free function  $f(u)$  where  $u = [(s - s_0)/s]^{1/2}$ . This function has been determined numerically. The only parameter  $A$  involved in this model affects the size of the discontinuity but not its form and it can be determined in each case from the width of the lowest member of the trajectory. The width function calculated is compared with the experimental widths. Consistency with exchange degeneracy is observed and discussed.

Finally the absorptive part along the left-hand cut is determined and plotted and a comparison with the phenomenological curves of other authors for the  $\rho$  trajectory is made.

In view of the differences among the curves of Fig. 4 we believe that a phenomenological analysis of the high-energy reactions, based on theoretical models for complex poles such as the one proposed, might be useful.

## ACKNOWLEDGMENTS

We wish to thank Dr. P. Deliyannis for discussions. One of us (N.G.A.) would like to thank D. Sotiriou for his help with the computational work.

## APPENDIX

We shall use a result of Sugawara and Tubis<sup>10</sup> in order to show that  $\alpha(s) \sim s$  for  $|s| \rightarrow \infty$ .

Consider a function  $f(z)$  with the following properties: (a)  $f(z)$  is analytic in  $z$  everywhere except for cuts which occur on the real axis and a finite number of poles; (b)  $f(z)$  is real in the sense that  $f(z)^* = f(z^*)$ ; (c)  $f(z)$  is bounded at  $|z| = \infty$  by a finite polynomial in  $z$ ; (d) the phase  $\delta(z)$  of  $f(z)$  (defined more precisely below) has finite limits  $\delta(\pm\infty)$  as  $z \rightarrow \pm\infty$ .

With the assumptions (a)–(d) it has been shown in (8) that for  $|z| \rightarrow \infty$

$$f(z) \sim z^{n-m} (-z)^{-\sigma/\pi} (z)^{\tau/\pi}, \quad (\text{A1})$$

where  $n$  and  $m$  are the number of zeros and poles of  $f(z)$ , respectively,

$$\sigma = \lim_{x \rightarrow +\infty} \delta(x), \quad \tau = \lim_{x \rightarrow -\infty} \delta(x). \quad (\text{A2})$$

The phase  $\delta(x)$  is defined by the relation

$$f(x+i\epsilon) = \pm |f(x+i\epsilon)| e^{i\delta(x)}$$

with the additional properties that  $\delta(x) = 0$  on the real axis where no cuts occur and has no discontinuities greater than or equal to  $\pi$  in magnitude. We now consider

$$f(s) \equiv \alpha(s) - N, \quad (\text{A3})$$

where  $N$  is an integer with the correct signature. Obviously  $f(s)$  satisfies (a), (b), and (c) above.

The function (A3) has no poles [by assumption (a) in Sec. II above] and no zeros on the first Riemann sheet of the  $s$  plane, since such zeros would correspond to particles with spin  $J = N$  which are allowed only on the second Riemann sheet. By the discussion of Ref. 10, the absence of zeros implies that assumption (d) is also satisfied. Hence (A1) and (A3) give

$$\alpha(s) \underset{|s| \rightarrow \infty}{\sim} (-s)^{-\sigma/\pi} (s)^{\tau/\pi}. \quad (\text{A4})$$

In our case, for  $s \geq s_0$ ,  $\text{Im} f(s) = \text{Im} \alpha(s) \geq 0$ ,  $\text{Im} f(s_0) = 0$ , and there exists a value  $\bar{s}$  of  $s$  in the interval  $(s_0, \infty)$  such that  $\text{Re} f(\bar{s}) = 0$ ,  $\text{Re} f(s) < 0$  for  $s_0 < s < \bar{s}$  and  $\text{Re} f(s) > 0$  for  $s > \bar{s}$ . We have also  $\delta(s_0) = 0$ . Then

$$-\pi \leq \delta(s) \leq 0 \quad \text{for } s > s_0$$

and

$$-\pi \leq \sigma \leq -\frac{1}{2}\pi. \quad (\text{A5})$$

Similarly, for  $s < 0$ ,  $\text{Im} f(0) = 0$  and  $\text{Re} f(s) < 0$ . Using also  $\delta(0) = 0$  we have  $-\frac{1}{2}\pi \leq \delta(s) \leq \frac{1}{2}\pi$  and, therefore,

$$-\frac{1}{2}\pi \leq \tau \leq \frac{1}{2}\pi. \quad (\text{A6})$$

By (A2) and (A4) we can write, for large positive  $s$ ,

$$\text{Re} \alpha(s) \sim \cos \left[ \lim_{s \rightarrow +\infty} \delta(s) \right] s^{\lim_{s \rightarrow \infty} [\delta(-s) - \delta(s)]/\pi}.$$

Since  $\text{Re} \alpha(s) \sim s$ , we have the following two possibilities:

$$\text{(I)} \quad \cos \left[ \lim_{s \rightarrow +\infty} \delta(s) \right] \neq 0$$

and

$$\lim_{s \rightarrow +\infty} [\delta(-s) - \delta(s)] = \pi;$$

$$\text{(II)} \quad \cos \left[ \lim_{s \rightarrow +\infty} \delta(s) \right] = 0$$

and

$$\lim_{s \rightarrow +\infty} [\delta(-s) - \delta(s)] > \pi.$$

However, case (II) must be excluded because, by (A5),

$$\cos\left[\lim_{s \rightarrow +\infty} \delta(s)\right] = 0$$

implies

$$\lim_{s \rightarrow +\infty} \delta(s) = \sigma = -\frac{1}{2}\pi.$$

Then by (A6)  $0 \leq \tau - \sigma \leq \pi$ , which is inconsistent with (II). Therefore  $\tau - \sigma = \pi$  and from (A4) we get  $\alpha(s) \sim s$ . This result along with the assumed linearity of the real part implies  $\text{Im}\alpha(s) \approx s$ .

These conclusions justify the fact that we have written once-subtracted dispersion relations in (2) and (3) of Sec. II.

\*On leave from Nuclear Research Center "Democritus," Aghia Paraskevi Attikis, Greece.

<sup>1</sup>J. S. Ball and F. Zachariassen, Phys. Rev. Letters **23**, 346 (1969); J. S. Ball, G. Marchesini, and F. Zachariassen, Phys. Letters **31B**, 583 (1970).

<sup>2</sup>R. Oehme, Phys. Rev. D **2**, 801 (1970).

<sup>3</sup>R. J. N. Phillips and V. Barger, Nucl. Phys. **33B**, 200 (1971).

<sup>4</sup>The presence of poles is obviously excluded because  $\alpha(s)$  must be bounded in the finite  $s$  plane. Otherwise the  $t$ -channel amplitude  $A(s, t) \approx t^{\text{Re}\alpha(s)}$  would not be polynomially bounded, which contradicts very general properties.

<sup>5</sup>A. O. Barut and D. E. Zwanziger, Phys. Rev. **127**, 974 (1962).

<sup>6</sup>P. D. B. Collins and E. J. Squires, in *Regge Poles*

in *Particle Physics*, edited by G. Höhler (Springer, Berlin, 1968), p. 73.

<sup>7</sup>It is well known from the theory of integral equations that if the square integrability of the solution is not required (i.e., if we allow  $\epsilon = 0$  exactly) then the solution of the integral equation (12) is not unique. Here we determine the unique  $L^2$  solution which will be seen to be physically acceptable because it gives rise to reasonable widths.

<sup>8</sup>B. R. Desai, P. Kaus, R. T. Park, and F. Zachariassen, Phys. Rev. Letters **25**, 1389 (1970); **25**, 1686(E) (1970).

<sup>9</sup>N. Barik, B. R. Desai, P. Kaus, and R. Park, Phys. Rev. D **4**, 2923 (1971).

<sup>10</sup>M. Sugawara and A. Tubis, Phys. Rev. **130**, 2127 (1963).

## Pion-Deuteron Scattering at High Energies\*

Deepinder P. Sidhu and C. Quigg

*Institute for Theoretical Physics, † State University of New York, Stony Brook, New York 11790*

(Received 31 August 1972)

Glauber theory, including the complications of spin and isospin, is applied to high-energy  $\pi d$  scattering. We compare theoretical predictions with recent experimental results on total and differential elastic cross sections. Particular attention is given to the suggestion of new experiments which bear on possible modifications of the Glauber picture.

### I. INTRODUCTION

The classic picture of high-energy hadron-nucleus collisions developed by Glauber<sup>1</sup> has by now reached a high degree of sophistication, and is well known to account for the basic features observed experimentally.<sup>2</sup> At the same time, Glauber theory has yet to be given a justification in terms of quantum field theory in the cloak of Feynman diagrams,<sup>3</sup> and periodic suggestions are made for its improvement. The history of the subject discourages the hope that a swift theoretical conclusion might be forthcoming, so we have undertaken a benchmark calculation of total and elas-

tic differential cross sections for  $\pi^+d$  scattering in terms of the "best available" pion-nucleon scattering amplitudes and deuteron wave functions. In so doing we have been able to make quantitative comparisons with recently published data and to recognize the need for additional experimental studies.

Our calculations of elastic differential cross sections represent in part merely an updating of earlier work by Michael and Wilkin<sup>4</sup> and by Alberi and Bertocchi.<sup>5</sup> In addition we treat briefly some modifications to Glauber theory proposed lately by Cheng and Wu.<sup>6</sup> A comparison of our calculated total cross sections with data obtained at Serpuk-